

hep-ph/0208092  
 UMN-TH-2108/02  
 TPI-MINN-02/25  
 August 2002

## SEARCHING FOR SUPERSYMMETRIC DARK MATTER\*

KEITH A. OLIVE

*Theoretical Physics Institute, School of Physics and Astronomy,  
 University of Minnesota, Minneapolis, MN 55455 USA  
 E-mail: olive@umn.edu*

Standard Model offers a promising cold dark matter candidate, the lightest neutralino. I will review the prospects for the detection of this candidate in both accelerator and direct detection searches.

### 1. Introduction

Although there are many reasons for considering supersymmetry as a candidate extension to the standard model of strong, weak and electromagnetic interactions<sup>1</sup>, one of the most compelling is its role in understanding the hierarchy problem<sup>2</sup> namely, why/how is  $m_W \ll M_P$ . One might think naively that it would be sufficient to set  $m_W \ll M_P$  by hand. However, radiative corrections tend to destroy this hierarchy. For example, one-loop diagrams generate

$$\delta m_W^2 = \mathcal{O}\left(\frac{\alpha}{\pi}\right) \Lambda^2 \gg m_W^2 \quad (1)$$

where  $\Lambda$  is a cut-off representing the appearance of new physics, and the inequality in (1) applies if  $\Lambda \sim 10^3$  TeV, and even more so if  $\Lambda \sim m_{GUT} \sim 10^{16}$  GeV or  $\sim M_P \sim 10^{19}$  GeV. If the radiative corrections to a physical quantity are much larger than its measured values, obtaining the latter requires strong cancellations, which in general require fine tuning of the bare input parameters. However, the necessary cancellations are natural in supersymmetry, where one has equal numbers of bosons  $B$  and fermions  $F$  with equal couplings, so that (1) is replaced by

$$\delta m_W^2 = \mathcal{O}\left(\frac{\alpha}{\pi}\right) |m_B^2 - m_F^2| . \quad (2)$$

The residual radiative correction is naturally small if  $|m_B^2 - m_F^2| \lesssim 1$  TeV<sup>2</sup>.

---

\*summary of invited talk at cospa 2002, 2002 international symposium on cosmology and particle astrophysics, may31 - june 2, 2002, national taiwan university taipei, taiwan.

In order to justify the absence of interactions which can be responsible for extremely rapid proton decay, it is common in the minimal supersymmetric standard model (MSSM) to assume the conservation of R-parity. If R-parity, which distinguishes between “normal” matter and the supersymmetric partners and can be defined in terms of baryon, lepton and spin as  $R = (-1)^{3B+L+2S}$ , is unbroken, there is at least one supersymmetric particle (the lightest supersymmetric particle or LSP) which must be stable. Thus, the minimal model contains the fewest number of new particles and interactions necessary to make a consistent theory.

There are very strong constraints, however, forbidding the existence of stable or long lived particles which are not color and electrically neutral<sup>3</sup>. Strong and electromagnetically interacting LSPs would become bound with normal matter forming anomalously heavy isotopes. Indeed, there are very strong upper limits on the abundances, relative to hydrogen, of nuclear isotopes<sup>4</sup>,  $n/n_H \lesssim 10^{-15}$  to  $10^{-29}$  for  $1 \text{ GeV} \lesssim m \lesssim 1 \text{ TeV}$ . A strongly interacting stable relic is expected to have an abundance  $n/n_H \lesssim 10^{-10}$  with a higher abundance for charged particles.

There are relatively few supersymmetric candidates which are not colored and are electrically neutral. The sneutrino<sup>5</sup> is one possibility, but in the MSSM, it has been excluded as a dark matter candidate by direct<sup>6</sup> and indirect<sup>7</sup> searches. In fact, one can set an accelerator based limit on the sneutrino mass from neutrino counting,  $m_{\tilde{\nu}} \gtrsim 44.7 \text{ GeV}$ <sup>8</sup>. In this case, the direct relic searches in underground low-background experiments require  $m_{\tilde{\nu}} \gtrsim 20 \text{ TeV}$ <sup>6</sup>. Another possibility is the gravitino which is probably the most difficult to exclude. I will concentrate on the remaining possibility in the MSSM, namely the neutralinos.

## 2. Parameters

The most general version of the MSSM, despite its minimality in particles and interactions contains well over a hundred new parameters. The study of such a model would be untenable were it not for some (well motivated) assumptions. These have to do with the parameters associated with supersymmetry breaking. It is often assumed that, at some unification scale, all of the gaugino masses receive a common mass,  $m_{1/2}$ . The gaugino masses at the weak scale are determined by running a set of renormalization group equations. Similarly, one often assumes that all scalars receive a common mass,  $m_0$ , at the GUT scale. These too are run down to the weak scale. The remaining parameters of importance involve the Higgs sector. There is the Higgs mixing mass parameter,  $\mu$ , and since there are two Higgs doublets in the MSSM, there are two vacuum expectation values. One combination

of these is related to the  $Z$  mass, and therefore is not a free parameter, while the other combination, the ratio of the two vevs,  $\tan\beta$ , is free.

If the supersymmetry breaking Higgs soft masses are also unified at the GUT scale (and take the common value  $m_0$ ), then  $\mu$  and the physical Higgs masses at the weak scale are determined by electroweak vacuum conditions. This scenario is often referred to as the constrained MSSM or CMSSM. Once these parameters are set, the entire spectrum of sparticle masses at the weak scale can be calculated.

### 3. Neutralinos

There are four neutralinos, each of which is a linear combination of the  $R = -1$  neutral fermions,<sup>3</sup>: the wino  $\tilde{W}^3$ , the partner of the 3rd component of the  $SU(2)_L$  gauge boson; the bino,  $\tilde{B}$ , the partner of the  $U(1)_Y$  gauge boson; and the two neutral Higgsinos,  $\tilde{H}_1$  and  $\tilde{H}_2$ . Assuming gaugino mass universality at the GUT scale, the identity and mass of the LSP are determined by the gaugino mass  $m_{1/2}$ ,  $\mu$ , and  $\tan\beta$ . In general, neutralinos can be expressed as a linear combination

$$\chi = \alpha \tilde{B} + \beta \tilde{W}^3 + \gamma \tilde{H}_1 + \delta \tilde{H}_2 \quad (3)$$

The solution for the coefficients  $\alpha, \beta, \gamma$  and  $\delta$  for neutralinos that make up the LSP can be found by diagonalizing the mass matrix

$$(\tilde{W}^3, \tilde{B}, \tilde{H}_1^0, \tilde{H}_2^0) \begin{pmatrix} M_2 & 0 & \frac{-g_2 v_1}{\sqrt{2}} & \frac{g_2 v_2}{\sqrt{2}} \\ 0 & M_1 & \frac{g_1 v_1}{\sqrt{2}} & \frac{-g_1 v_2}{\sqrt{2}} \\ \frac{-g_2 v_1}{\sqrt{2}} & \frac{g_1 v_1}{\sqrt{2}} & 0 & -\mu \\ \frac{g_2 v_2}{\sqrt{2}} & \frac{-g_1 v_2}{\sqrt{2}} & -\mu & 0 \end{pmatrix} \begin{pmatrix} \tilde{W}^3 \\ \tilde{B} \\ \tilde{H}_1^0 \\ \tilde{H}_2^0 \end{pmatrix} \quad (4)$$

where  $M_1 (M_2)$  is a soft supersymmetry breaking term giving mass to the  $U(1)$  ( $SU(2)$ ) gaugino(s). In a unified theory  $M_1 = M_2$  at the unification scale (at the weak scale,  $M_1 \simeq \frac{5}{3} \frac{\alpha_1}{\alpha_2} M_2$ ). As one can see, the coefficients  $\alpha, \beta, \gamma$ , and  $\delta$  depend only on  $m_{1/2}$ ,  $\mu$ , and  $\tan\beta$ .

In Figure 1<sup>9</sup>, regions in the  $M_2, \mu$  plane with  $\tan\beta = 2$  are shown in which the LSP is one of several nearly pure states, the photino,  $\tilde{\gamma}$ , the bino,  $\tilde{B}$ , a symmetric combination of the Higgsinos,  $\tilde{H}_{(12)}$ , or the Higgsino,  $\tilde{S} = \sin\beta \tilde{H}_1 + \cos\beta \tilde{H}_2$ . The dashed lines show the LSP mass contours. The cross hatched regions correspond to parameters giving a chargino ( $\tilde{W}^\pm, \tilde{H}^\pm$ ) state with mass  $m_{\tilde{\chi}} \leq 45\text{GeV}$  and as such are excluded by LEP<sup>10</sup>. This constraint has been extended by LEP<sup>11</sup> and is shown by the light shaded region and corresponds to regions where the chargino mass is  $\lesssim 104$  GeV. The newer limit does not extend deep into the Higgsino region because

of the degeneracy between the chargino and neutralino. Notice that the parameter space is dominated by the  $\tilde{B}$  or  $\tilde{H}_{12}$  pure states and that the photino only occupies a small fraction of the parameter space, as does the Higgsino combination  $\tilde{S}$ . Both of these light states are experimentally excluded.

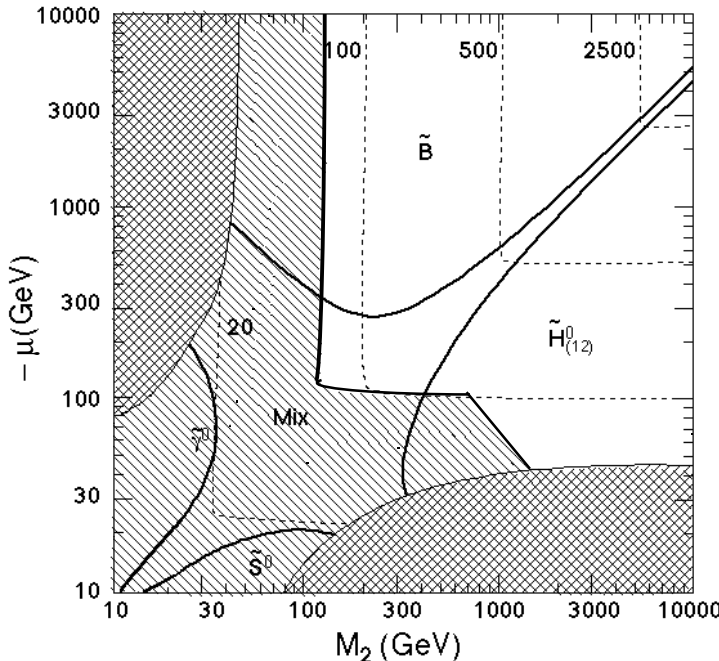


Figure 1. Mass contours and composition of nearly pure LSP states in the MSSM <sup>9</sup>.

#### 4. The Relic Density

The relic abundance of LSP's is determined by solving the Boltzmann equation for the LSP number density in an expanding Universe. The technique<sup>12</sup> used is similar to that for computing the relic abundance of massive neutrinos<sup>13</sup>. The relic density depends on additional parameters in the MSSM beyond  $m_{1/2}$ ,  $\mu$ , and  $\tan\beta$ . These include the sfermion masses,  $m_{\tilde{f}}$  and the Higgs pseudo-scalar mass,  $m_A$ <sup>a</sup>, derived from  $m_0$  (and  $m_{1/2}$ ).

<sup>a</sup>In general, the relic density depends on the supersymmetry-breaking tri-linear masses  $A$  (also assumed to be unified at the GUT scale) as well as two phases  $\theta_\mu$  and  $\theta_A$ .

To determine the relic density it is necessary to obtain the general annihilation cross-section for neutralinos. In much of the parameter space of interest, the LSP is a bino and the annihilation proceeds mainly through sfermion exchange. Because of the p-wave suppression associated with Majorana fermions, the s-wave part of the annihilation cross-section is suppressed by the outgoing fermion masses. This means that it is necessary to expand the cross-section to include p-wave corrections which can be expressed as a term proportional to the temperature if neutralinos are in equilibrium. Unless the neutralino mass happens to lie near a pole, such as  $m_\chi \simeq m_Z/2$  or  $m_h/2$ , in which case there are large contributions to the annihilation through direct  $s$ -channel resonance exchange, the dominant contribution to the  $\tilde{B}\tilde{B}$  annihilation cross section comes from crossed  $t$ -channel sfermion exchange.

Annihilations in the early Universe continue until the annihilation rate  $\Gamma \simeq \sigma v n_\chi$  drops below the expansion rate given by the Hubble parameter,  $H$ . For particles which annihilate through approximate weak scale interactions, this occurs when  $T \sim m_\chi/20$ . Subsequently, the relic density of neutralinos is fixed relative to the number of relativistic particles. As noted above, the number density of neutralinos is tracked by a Boltzmann-like equation,

$$\frac{dn}{dt} = -3 \frac{\dot{R}}{R} n - \langle \sigma v \rangle (n^2 - n_0^2) \quad (5)$$

where  $n_0$  is the equilibrium number density of neutralinos. By defining the quantity  $f = n/T^3$ , we can rewrite this equation in terms of  $x$ , as

$$\frac{df}{dx} = m_\chi \left( \frac{1}{90} \pi^2 \kappa^2 N \right)^{1/2} (f^2 - f_0^2) \quad (6)$$

The solution to this equation at late times (small  $x$ ) yields a constant value of  $f$ , so that  $n \propto T^3$ . The final relic density expressed as a fraction of the critical energy density can be written as<sup>3</sup>

$$\Omega_\chi h^2 \simeq 1.9 \times 10^{-11} \left( \frac{T_\chi}{T_\gamma} \right)^3 N_f^{1/2} \left( \frac{\text{GeV}}{ax_f + \frac{1}{2}bx_f^2} \right) \quad (7)$$

where  $(T_\chi/T_\gamma)^3$  accounts for the subsequent reheating of the photon temperature with respect to  $\chi$ , due to the annihilations of particles with mass  $m < x_f m_\chi$ <sup>14</sup>. The subscript  $f$  refers to values at freeze-out, i.e., when annihilations cease. The coefficients  $a$  and  $b$  are related to the partial wave expansion of the cross-section,  $\sigma v = a + bx + \dots$ . Eq. (7) results in a very good approximation to the relic density expect near s-channel annihilation

poles, thresholds and in regions where the LSP is nearly degenerate with the next lightest supersymmetric particle<sup>15</sup>.

## 5. Phenomenological and Cosmological Constraints

For the cosmological limits on the relic density I will assume

$$0.1 \leq \Omega_\chi h^2 \leq 0.3. \quad (8)$$

The upper limit being a conservative bound based only on the lower limit to the age of the Universe of 12 Gyr. Indeed, most analyses indicate that  $\Omega_{\text{matter}} \lesssim 0.4 - 0.5$  and thus it is very likely that  $\Omega_\chi h^2 < 0.2$ . One should note that smaller values of  $\Omega_\chi h^2$  are allowed, since it is quite possible that some of the cold dark matter might not consist of LSPs.

The calculated relic density is found to have a relevant cosmological density over a wide range of susy parameters. For all values of  $\tan\beta$ , there is a ‘bulk’ region with relatively low values of  $m_{1/2}$  and  $m_0$  where  $0.1 < \Omega_\chi h^2 < 0.3$ . However there are a number of regions at large values of  $m_{1/2}$  and/or  $m_0$  where the relic density is still compatible with the cosmological constraints. At large values of  $m_{1/2}$ , the lighter stau, becomes nearly degenerate with the neutralino and co-annihilations between these particles must be taken into account<sup>16</sup>. For non-zero values of  $A_0$ , there are new regions for which  $\chi - \tilde{t}$  coannihilations are important<sup>17</sup>. At large  $\tan\beta$ , as one increases  $m_{1/2}$ , the pseudo-scalar mass,  $m_A$  begins to drop so that there is a wide funnel-like region (at all values of  $m_0$ ) such that  $2m_\chi \approx m_A$  and s-channel annihilations become important<sup>18,19</sup>. Finally, there is a region at very high  $m_0$  where the value of  $\mu$  begins to fall and the LSP becomes more Higgsino-like. This is known as the ‘focus point’ region<sup>20</sup>.

As an aid to the assessment of the prospects for detecting sparticles at different accelerators, benchmark sets of supersymmetric parameters have often been found useful, since they provide a focus for concentrated discussion. A set of proposed post-LEP benchmark scenarios<sup>21</sup> in the CMSSM are illustrated schematically in Fig. 2. Five of the chosen points are in the ‘bulk’ region at small  $m_{1/2}$  and  $m_0$ , four are spread along the coannihilation ‘tail’ at larger  $m_{1/2}$  for various values of  $\tan\beta$ . This tail runs along the shaded region in the lower right corner where the stau is the LSP and is therefore excluded by the constraints against charged dark matter. Two points are in rapid-annihilation ‘funnels’ at large  $m_{1/2}$  and  $m_0$ . At large values of  $m_0$ , the focus-point region runs along the boundary where electroweak symmetry no longer occurs (shown in Fig. 2 as the shaded region in the upper left corner). Two points were chosen in the focus-point region

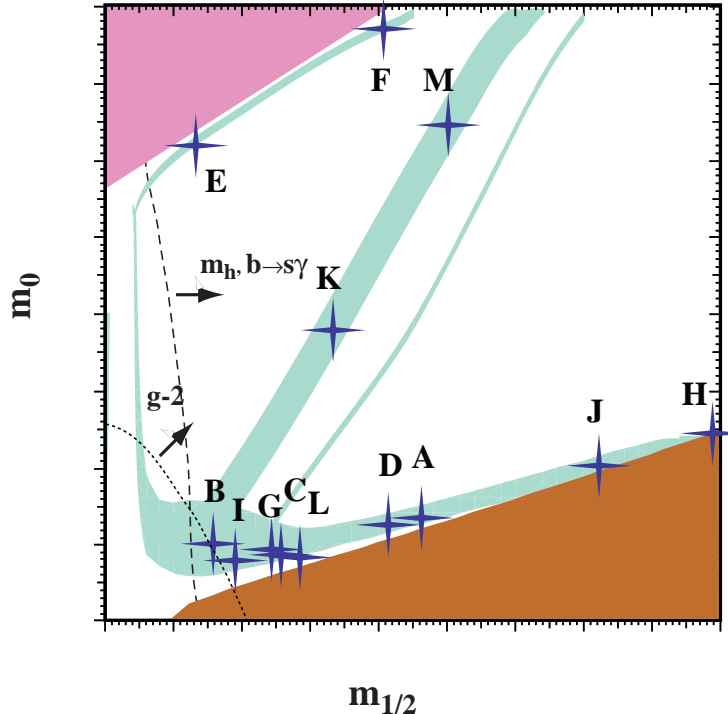


Figure 2. Schematic overview of the CMSSM benchmark points proposed in <sup>21</sup>. The points are intended to illustrate the range of available possibilities. The labels correspond to the approximate positions of the benchmark points in the  $(m_{1/2}, m_0)$  plane. They also span values of  $\tan \beta$  from 5 to 50 and include points with  $\mu < 0$ .

at large  $m_0$ . The proposed points range over the allowed values of  $\tan \beta$  between 5 and 50. The light shaded region corresponds to the portion of parameter space where the relic density  $\Omega_\chi h^2$  is between 0.1 and 0.3.

The most important phenomenological constraints are also shown schematically in Figure 2. These include the constraint provided by the LEP lower limit on the Higgs mass:  $m_H > 114.1$  GeV <sup>22</sup>. This holds in the Standard Model, for the lightest Higgs boson  $h$  in the general MSSM for  $\tan \beta \lesssim 8$ , and almost always in the CMSSM for all  $\tan \beta$ . Since  $m_h$  is sensitive to sparticle masses, particularly  $m_{\tilde{t}}$ , via loop corrections, the Higgs limit also imposes important constraints on the CMSSM parameters, principally  $m_{1/2}$  as seen by the dashed curve in Fig. 2. The constraint imposed by measurements of  $b \rightarrow s\gamma$  <sup>23</sup> also exclude small values of  $m_{1/2}$ . These measurements agree with the Standard Model, and therefore pro-

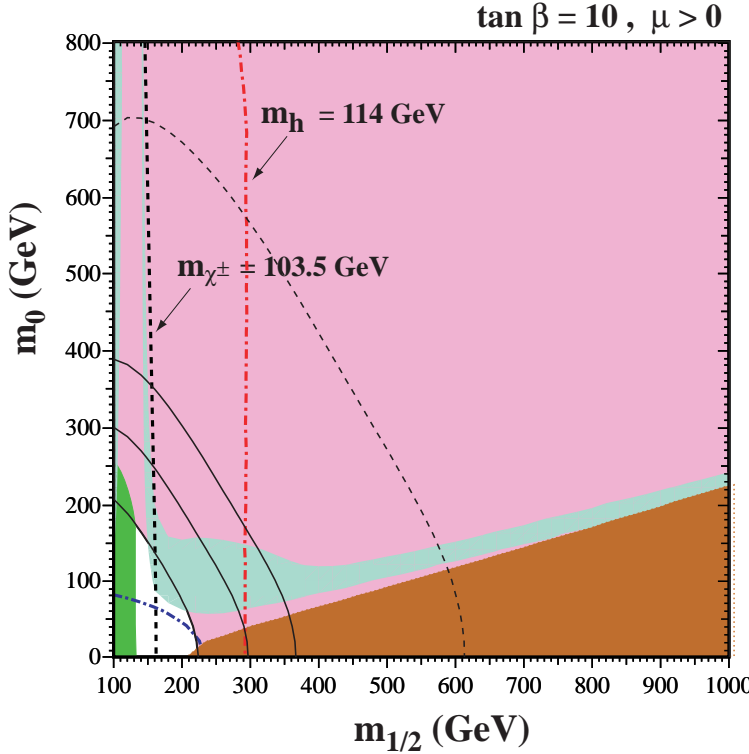


Figure 3. Compilation of phenomenological constraints on the CMSSM for  $\tan \beta = 10, \mu > 0$ , assuming  $A_0 = 0, m_t = 175$  GeV and  $m_b(m_b)_{SM}^{\overline{MS}} = 4.25$  GeV. The near-vertical lines are the LEP limits  $m_{\chi^\pm} = 103.5$  GeV (dashed and black)<sup>11</sup>, and  $m_h = 114.1$  GeV (dotted and red)<sup>22</sup>. Also, in the lower left corner we show the  $m_{\tilde{e}} = 99$  GeV contour<sup>28</sup>. In the dark (brick red) shaded regions, the LSP is the charged  $\tilde{\tau}_1$ , so this region is excluded. The light(turquoise) shaded areas are the cosmologically preferred regions with  $0.1 \leq \Omega h^2 \leq 0.3$ <sup>19</sup>. The medium (dark green) shaded regions are excluded by  $b \rightarrow s\gamma$ <sup>23</sup>. The shaded (pink) region in the upper right delineates the  $2\sigma$  range of  $g_\mu - 2$ .

vide bounds on MSSM particles, such as the chargino and charged Higgs masses, in particular. Typically, the  $b \rightarrow s\gamma$  constraint is more important for  $\mu < 0$ , but it is also relevant for  $\mu > 0$ , particularly when  $\tan \beta$  is large. The BNL E821 experiment reported last year a new measurement of  $a_\mu \equiv \frac{1}{2}(g_\mu - 2)$  which deviated by 2.6 standard deviations from the best Standard Model prediction available at that time<sup>24</sup>. The largest contribution to the errors in the comparison with theory was thought to be the statistical error of the experiment, which has been significantly re-

duced just recently<sup>25</sup>. However, it has recently been realized that the sign of the most important pseudoscalar-meson pole part of the light-by-light scattering contribution<sup>26</sup> to the Standard Model prediction should be reversed, which reduces the apparent experimental discrepancy to about 1.6 standard deviations ( $\delta a_\mu \times 10^{10} = 26 \pm 16$ ). With the new data, the discrepancy with theory ranges from 1.6 to 2.6  $\sigma$ , i.e.,  $\delta a_\mu \times 10^{10} = 26 \pm 10$  to  $17 \pm 11$ <sup>25</sup>. This constraint excludes very small values of  $m_{1/2}$  and  $m_0$ . In Fig. 2, the  $g - 2$  constraint is shown schematically by the dotted line. It may also exclude very large values of the parameters as well as negative values of  $\mu$ , if the discrepancy holds up.

Following a previous analysis<sup>27</sup>, in Figure 3 the  $m_{1/2} - m_0$  parameter space is shown for  $\tan \beta = 10$ . The dark shaded region (in the lower right) corresponds to the parameters where the LSP is not a neutralino but rather a  $\tilde{\tau}_R$ . The cosmologically interesting region at the left of the figure is due to the appearance of pole effects. There, the LSP can annihilate through s-channel  $Z$  and  $h$  (the light Higgs) exchange, thereby allowing a very large value of  $m_0$ . However, this region is excluded by phenomenological constraints. Here one can see clearly the coannihilation tail which extends towards large values of  $m_{1/2}$ . In addition to the phenomenological constraints discussed above, Figure 3 also shows the current experimental constraints on the CMSSM parameter space due to the limit  $m_{\chi^\pm} \gtrsim 103.5$  GeV provided by chargino searches at LEP<sup>11</sup>. LEP has also provided lower limits on slepton masses, of which the strongest is  $m_{\tilde{e}} \gtrsim 99$  GeV<sup>28</sup>. This is shown by dot-dashed curve in the lower left corner of Fig. 3.

As one can see, one of the most important phenomenological constraint at this value of  $\tan \beta$  is due to the Higgs mass (shown by the nearly vertical dot-dashed curve). The theoretical Higgs masses were evaluated using **FeynHiggs**<sup>29</sup>, which is estimated to have a residual uncertainty of a couple of GeV in  $m_h$ . The region excluded by the  $b \rightarrow s\gamma$  constraint is the dark shaded (green) region to the left of the plot.

As many authors have pointed out<sup>30</sup>, a discrepancy between theory and the BNL experiment could well be explained by supersymmetry. As seen in Fig. 3, this is particularly easy if  $\mu > 0$ . The medium (pink) shaded region in the figure corresponds to the overall allowed region by the new experimental result:  $-5 < \delta a_\mu \times 10^{10} < 46$ . The two solid lines within the shaded region corresponds to the central values  $\delta a_\mu \times 10^{10} = 17$  and  $26$  respectively. The optimistic  $2\sigma$  lower bound of  $\delta a_\mu \times 10^{10} = 6$  is shown as a dashed curve.

As discussed above, another mechanism for extending the allowed CMSSM region to large  $m_\chi$  is rapid annihilation via a direct-channel pole

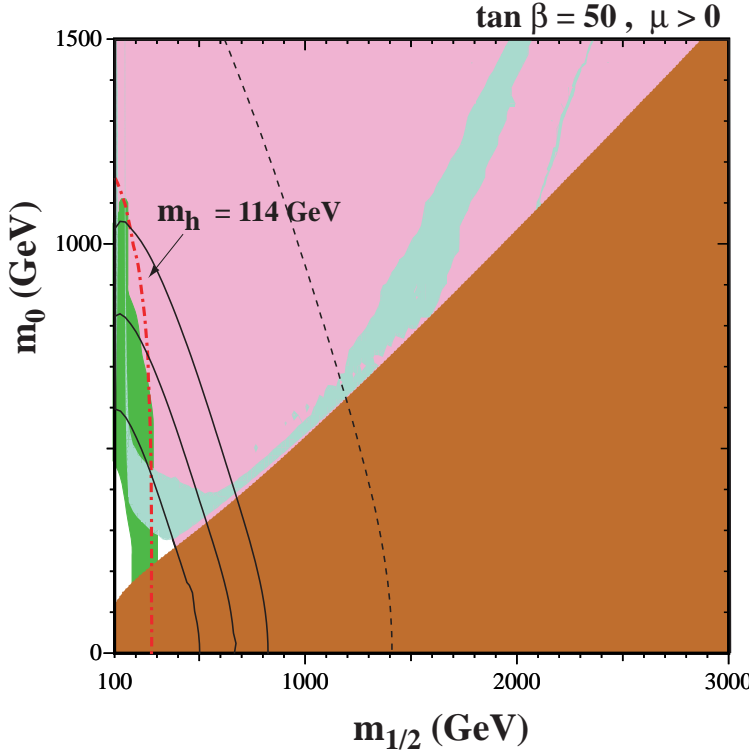


Figure 4. As in Fig. 3 for  $\tan \beta = 50$ .

when  $m_\chi \sim \frac{1}{2}m_A$ <sup>18,19</sup>. This may yield a ‘funnel’ extending to large  $m_{1/2}$  and  $m_0$  at large  $\tan \beta$ , as seen in Fig. 4.

In principle the true input parameters in the CMSSM are:  $\mu, m_1, m_2$ , and  $B$ , where  $m_1$  and  $m_2$  are the Higgs soft masses (in the CMSSM  $m_1 = m_2 = m_0$  and  $B$  is the susy breaking bilinear mass term). In this case, the electroweak symmetry breaking conditions lead to a prediction of  $M_Z, \tan \beta$ , and  $m_A$ . Since we are not really interested in predicting  $M_Z$ , it is more useful to assume instead the following CMSSM input parameters:  $M_Z, m_1, m_2$ , and  $\tan \beta$  again with  $m_1 = m_2 = m_0$ . In this case, one predicts  $\mu, B$ , and  $m_A$ . However, one can generalize the CMSSM case to include non-universal Higgs masses (NUHM), in which case the input parameters become:  $M_Z, \mu, m_A$ , and  $\tan \beta$  and one predicts  $m_1, m_2$ , and  $B$ .

The NUHM parameter space was recently analyzed<sup>31</sup> and a sample of the results found is shown in Fig. 5. While much of the cosmologically

preferred area with  $\mu < 0$  is excluded, there is a significant enhancement in the allowed parameter space for  $\mu > 0$ .

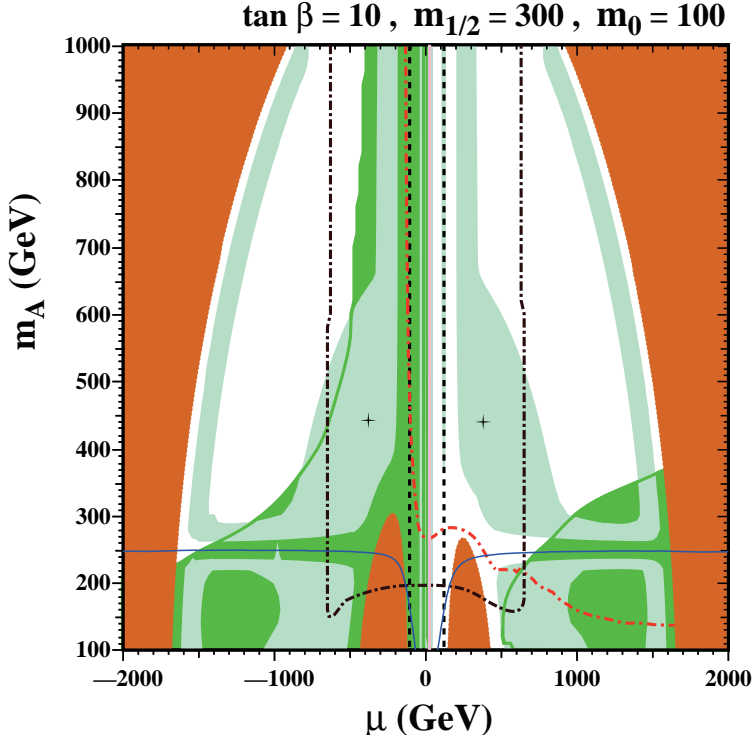


Figure 5. Compilations of phenomenological constraints on the MSSM with NUHM in the  $(\mu, m_A)$  plane for  $\tan \beta = 10$  and  $m_0 = 100$  GeV,  $m_{1/2} = 300$  GeV, assuming  $A_0 = 0$ ,  $m_t = 175$  GeV and  $m_b(m_b)_{SM}^{\overline{MS}} = 4.25$  GeV. The shading is as described in Fig. 3. The (blue) solid line is the contour  $m_\chi = m_A/2$ , near which rapid direct-channel annihilation suppresses the relic density. The dark (black) dot-dashed line indicates when one or another Higgs mass-squared becomes negative at the GUT scale: only lower  $|\mu|$  and larger  $m_A$  values are allowed. The crosses denote the values of  $\mu$  and  $m_A$  found in the CMSSM.

### 5.1. *Detection*

Because the LSP as dark matter is present locally, there are many avenues for pursuing dark matter detection. Direct detection techniques rely on an ample neutralino-nucleon scattering cross-section. The effective four-

fermion lagrangian can be written as

$$\begin{aligned}\mathcal{L} = & \bar{\chi} \gamma^\mu \gamma^5 \chi \bar{q}_i \gamma_\mu (\alpha_{1i} + \alpha_{2i} \gamma^5) q_i \\ & + \alpha_{3i} \bar{\chi} \chi \bar{q}_i q_i + \alpha_{4i} \bar{\chi} \gamma^5 \chi \bar{q}_i \gamma^5 q_i \\ & + \alpha_{5i} \bar{\chi} \chi \bar{q}_i \gamma^5 q_i + \alpha_{6i} \bar{\chi} \gamma^5 \chi \bar{q}_i q_i\end{aligned}\quad (9)$$

However, the terms involving  $\alpha_{1i}$ ,  $\alpha_{4i}$ ,  $\alpha_{5i}$ , and  $\alpha_{6i}$  lead to velocity dependent elastic cross sections. The remaining terms are: the spin dependent coefficient,  $\alpha_{2i}$  and the scalar coefficient  $\alpha_{3i}$ . Contributions to  $\alpha_{2i}$  are predominantly through light squark exchange. This is the dominant channel for binos. Scattering also occurs through Z exchange but this channel requires a strong Higgsino component. Contributions to  $\alpha_{3i}$  are also dominated by light squark exchange but Higgs exchange is non-negligible in most cases.

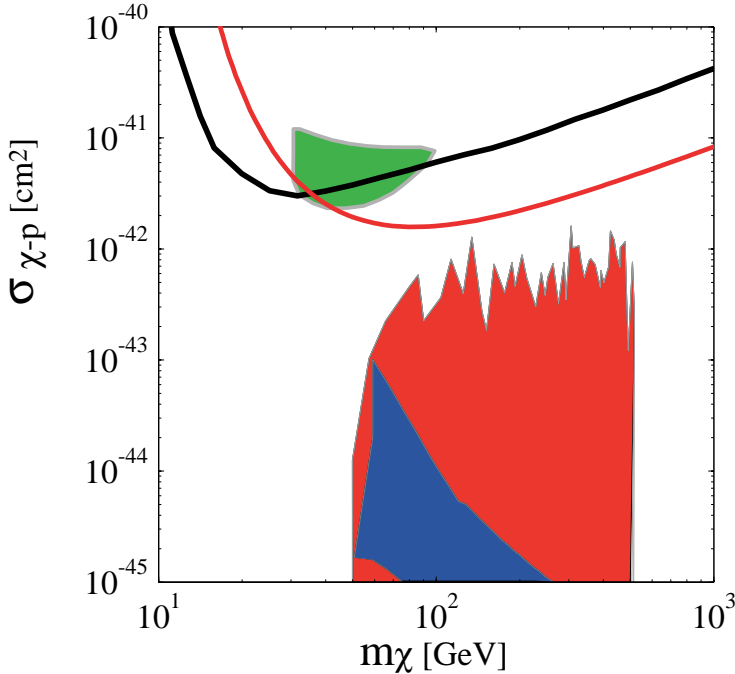


Figure 6. Limits from the CDMS <sup>34</sup> and Edelweiss <sup>35</sup> experiments on the neutralino-proton elastic scattering cross section as a function of the neutralino mass. The Edelweiss limit is stronger at higher  $m_\chi$ . These results nearly exclude the shaded region observed by DAMA <sup>36</sup>. The theoretical predictions lie at lower values of the cross section.

The results from a CMSSM and MSSM analysis<sup>32,33</sup> for  $\tan \beta = 3$  and 10 are compared with the most recent CDMS<sup>34</sup> and Edelweiss<sup>35</sup> bounds in Fig. 6. These results have nearly entirely excluded the region purported by the DAMA<sup>36</sup> experiment. The CMSSM prediction<sup>32</sup> is shown by the dark shaded region, while the NUHM case<sup>33</sup> is shown by the larger lighter shaded region.

I conclude by showing the prospects for direct detection for the benchmark points discussed above<sup>37</sup>. Fig. 7 shows rates for the elastic spin-independent scattering of supersymmetric relics, including the projected sensitivities for CDMS II<sup>38</sup> and CRESST<sup>39</sup> (solid) and GENIUS<sup>40</sup> (dashed). Also shown are the cross sections calculated in the proposed benchmark scenarios discussed in the previous section, which are considerably below the DAMA<sup>36</sup> range ( $10^{-5} - 10^{-6}$  pb). Indirect searches for supersymmetric dark matter via the products of annihilations in the galactic halo or inside the Sun also have prospects in some of the benchmark scenarios<sup>37</sup>.

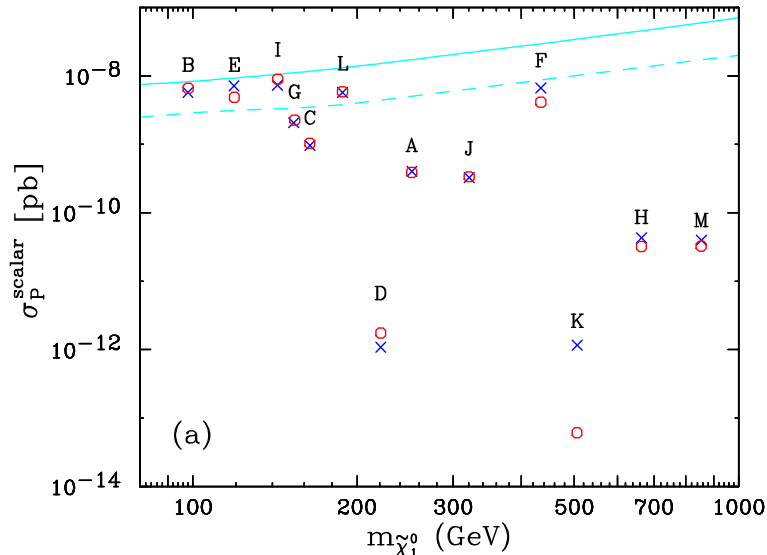


Figure 7. Elastic spin-independent scattering of supersymmetric relics on protons calculated in benchmark scenarios<sup>37</sup>, compared with the projected sensitivities for CDMS II<sup>38</sup> and CRESST<sup>39</sup> (solid) and GENIUS<sup>40</sup> (dashed). The predictions of our code (blue crosses) and `Neutdriver`<sup>41</sup> (red circles) for neutralino-nucleon scattering are compared. The labels A, B, ..., L correspond to the benchmark points as shown in Fig. 2.

### Acknowledgments

I would like to thank J. Ellis, T. Falk, A. Ferstl, G. Ganis, Y. Santoso, and M. Srednicki for enjoyable collaborations from which this work is culled. This work was supported in part by DOE grant DE-FG02-94ER40823 at Minnesota.

### References

1. J. Wess and J. Bagger, *Supersymmetry and Supergravity*, (Princeton University Press, Princeton NJ, 1992);  
G.G. Ross, *Grand Unified Theories*, (Addison-Wesley, Redwood City CA, 1985);  
S. Martin, arXiv:hep-ph/9709356;  
J. Ellis, arXiv:hep-ph/9812235;  
K.A. Olive, arXiv:hep-ph/9911307 .
2. L. Maiani, *Proceedings of the 1979 Gif-sur-Yvette Summer School On Particle Physics*, 1;  
G. 't Hooft, in *Recent Developments in Gauge Theories, Proceedings of the Nato Advanced Study Institute, Cargese, 1979*, eds. G. 't Hooft et al., (Plenum Press, NY, 1980);  
E. Witten, *Phys. Lett.* **B105**, 267 (1981).
3. J. Ellis, J.S. Hagelin, D.V. Nanopoulos, K.A. Olive and M. Srednicki, *Nucl. Phys.* **B238**, 453 (1984);  
see also H. Goldberg, *Phys. Rev. Lett.* **50**, 1419 (1983).
4. J. Rich, M. Spiro and J. Lloyd-Owen, *Phys. Rep.* **151**, 239 (1987);  
P.F. Smith, *Contemp. Phys.* **29**, 159 (1998);  
T.K. Hemmick et al., *Phys. Rev.* **D41**, 2074 (1990).
5. L.E. Ibanez, *Phys. Lett.* **137B**, 160 (1984);  
J. Hagelin, G.L. Kane, and S. Raby, *Nucl., Phys.* **B241**, 638 (1984);  
T. Falk, K.A. Olive, and M. Srednicki, *Phys. Lett.* **B339**, 248 (1994).
6. S. Ahlen, et. al., *Phys. Lett.* **B195**, 603 (1987);  
D.D. Caldwell, et. al., *Phys. Rev. Lett.* **61**, 510 (1988);  
M. Beck et al., *Phys. Lett.* **B336** 141 (1994).
7. see e.g. K.A. Olive and M. Srednicki, *Phys. Lett.* **205B**, 553 (1988).
8. The LEP Collaborations, the LEP Electroweak Working Group, and the SLD Heavy Flavour and Electroweak Groups, CERN-EP-2000-016.
9. K.A. Olive and M. Srednicki, *Phys. Lett.* **B230**, 78 (1989); *Nucl. Phys.* **B355**, 208 (1991).
10. ALEPH collaboration, D. Decamp et al., *Phys. Rep.* **216**, 253 (1992);  
L3 collaboration, M. Acciarri et al., *Phys. Lett.* **B350**, 109 (1995);  
OPAL collaboration, G. Alexander et al., *Phys. Lett.* **B377**, 273 (1996).
11. Joint LEP 2 Supersymmetry Working Group, *Combined LEP Chargino Results, up to 208 GeV*,  
[http://lepsusy.web.cern.ch/lepsusy/www/inos\\_moriond01/charginos\\_pub.html](http://lepsusy.web.cern.ch/lepsusy/www/inos_moriond01/charginos_pub.html).
12. R. Watkins, M. Srednicki and K.A. Olive, *Nucl. Phys.* **B310**, 693 (1988).
13. P. Hut, *Phys. Lett.* **69B**, 85 (1977);

- B.W. Lee and S. Weinberg, *Phys. Rev. Lett.* **39**, 165 (1977).
14. G. Steigman, K. A. Olive and D. N. Schramm, *Phys. Rev. Lett.* **43**, 239 (1979);  
 K. A. Olive, D. N. Schramm and G. Steigman, *Nucl. Phys. B* **180**, 497 (1981).
15. K. Griest and D. Seckel, *Phys. Rev. D* **43**, 3191 (1991).
16. J. Ellis, T. Falk, and K. Olive, *Phys. Lett. B* **444**, 367 (1998);  
 J. Ellis, T. Falk, K. Olive, and M. Srednicki, *Astr. Part. Phys.* (in **13**, 181 (2000) [Erratum-*ibid.* **15**, 413 (2000)]; M. E. Gómez, G. Lazarides and C. Pallis, *Phys. Rev. D* **61** (2000) 123512 and *Phys. Lett. B* **487** (2000) 313;  
 R. Arnowitt, B. Dutta and Y. Santoso, *Nucl. Phys. B* **606** (2001) 59.
17. C. Boehm, A. Djouadi and M. Drees, *Phys. Rev. D* **62**, 035012 (2000);  
 J. Ellis, K.A. Olive and Y. Santoso, arXiv:hep-ph/0112113.
18. M. Drees and M. M. Nojiri, *Phys. Rev. D* **47**, 376 (1993);  
 H. Baer and M. Brhlik, *Phys. Rev. D* **53**, 597 (1996) ;and *Phys. Rev. D* **57** 567 (1998);  
 H. Baer, M. Brhlik, M. A. Diaz, J. Ferrandis, P. Mercadante, P. Quintana and X. Tata, *Phys. Rev. D* **63**, 015007 (2001);  
 A. B. Lahanas, D. V. Nanopoulos and V. C. Spanos, *Mod. Phys. Lett. A* **16** 1229 (2001).
19. J. R. Ellis, T. Falk, G. Ganis, K. A. Olive and M. Srednicki, *Phys. Lett. B* **510**, 236 (2001).
20. J. L. Feng, K. T. Matchev and T. Moroi, *Phys. Rev. Lett.* **84**, 2322 (2000);  
 J. L. Feng, K. T. Matchev and T. Moroi, *Phys. Rev. D* **61**, 075005 (2000);  
 J. L. Feng, K. T. Matchev and F. Wilczek, *Phys. Lett. B* **482**, 388 (2000).
21. M. Battaglia et al., *Eur. Phys. J. C* **22** 535 (2001).
22. LEP Higgs Working Group for Higgs boson searches, OPAL Collaboration, ALEPH Collaboration, DELPHI Collaboration and L3 Collaboration, *Search for the Standard Model Higgs Boson at LEP*, ALEPH-2001-066, DELPHI-2001-113, CERN-L3-NOTE-2699, OPAL-PN-479, LHWG-NOTE-2001-03, CERN-EP/2001-055, arXiv:hep-ex/0107029; *Searches for the neutral Higgs bosons of the MSSM: Preliminary combined results using LEP data collected at energies up to 209 GeV*, LHWG-NOTE-2001-04, ALEPH-2001-057, DELPHI-2001-114, L3-NOTE-2700, OPAL-TN-699, arXiv:hep-ex/0107030.
23. M.S. Alam et al., [CLEO Collaboration], *Phys. Rev. Lett.* **74**, 2885 (1995);  
 as updated in S. Ahmed et al., CLEO CONF 99-10; BELLE Collaboration, BELLE-CONF-0003, contribution to the 30th International conference on High-Energy Physics, Osaka, 2000;  
 See also K. Abe et al., [Belle Collaboration], [arXiv:hep-ex/0107065];  
 L. Lista [BaBar Collaboration], [arXiv:hep-ex/0110010];  
 C. Degrandi, P. Gambino and G. F. Giudice, *JHEP* **0012**, 009 (2000);  
 M. Carena, D. Garcia, U. Nierste and C. E. Wagner, *Phys. Lett. B* **499**, 141 (2001);  
 P. Gambino and M. Misiak, *Nucl. Phys. B* **611** (2001) 338;  
 D. A. Demir and K. A. Olive, *Phys. Rev. D* **65**, 034007 (2002).
24. H. N. Brown et al. [Muon g-2 Collaboration], *Phys. Rev. Lett.* **86**, 2227 (2001).
25. G.W. Bennet et al. [Muon g-2 Collaboration], arXiv:hep-ex/0208001.

26. M. Knecht and A. Nyffeler, *Phys. Rev. D* **65**, 073034 (2002);  
 M. Knecht, A. Nyffeler, M. Perrottet and E. De Rafael, *Phys. Rev. Lett.* **88**, 071802 (2002);  
 M. Hayakawa and T. Kinoshita, arXiv:hep-ph/0112102;  
 I. Blokland, A. Czarnecki and K. Melnikov, *Phys. Rev. Lett.* **88**, 071803 (2002);  
 J. Bijnens, E. Pallante and J. Prades, *Nucl. Phys. B* **626**, 410 (2002).
27. J. R. Ellis, K. A. Olive and Y. Santoso, *New Jour. Phys.* **4**, 32 (2002).
28. Joint LEP 2 Supersymmetry Working Group, *Combined LEP Selec-tron/Smuon/Stau Results, 183-208 GeV*,  
<http://alephwww.cern.ch/~ganis/SUSYWG/SLEP/sleptons.2k01.html>.
29. S. Heinemeyer, W. Hollik and G. Weiglein, *Comput. Phys. Commun.* **124**, 76 (2000);  
 S. Heinemeyer, W. Hollik and G. Weiglein, *Eur. Phys. J. C* **9**, 343 (1999).
30. L. L. Everett, G. L. Kane, S. Rigolin and L. Wang, *Phys. Rev. Lett.* **86**, 3484 (2001);  
 J. L. Feng and K. T. Matchev, *Phys. Rev. Lett.* **86**, 3480 (2001);  
 E. A. Baltz and P. Gondolo, *Phys. Rev. Lett.* **86**, 5004 (2001);  
 U. Chattopadhyay and P. Nath, *Phys. Rev. Lett.* **86**, 5854 (2001);  
 S. Komine, T. Moroi and M. Yamaguchi, *Phys. Lett. B* **506**, 93 (2001);  
 J. Ellis, D. V. Nanopoulos and K. A. Olive, *Phys. Lett. B* **508**, 65 (2001);  
 R. Arnowitt, B. Dutta, B. Hu and Y. Santoso, *Phys. Lett. B* **505**, 177 (2001);  
 S. P. Martin and J. D. Wells, *Phys. Rev. D* **64**, 035003 (2001);  
 H. Baer, C. Balazs, J. Ferrandis and X. Tata, *Phys. Rev. D* **64**, 035004 (2001).
31. J. Ellis, K. Olive and Y. Santoso, *Phys. Lett. B* **539**, 107 (2002).
32. J. R. Ellis, A. Ferstl and K. A. Olive, *Phys. Lett. B* **481**, 304 (2000); see also:  
*Phys. Lett. B* **532**, 318 (2002).
33. J. R. Ellis, A. Ferstl and K. A. Olive, *Phys. Rev. D* **63**, 065016 (2001).
34. D. Abrams *et al.* [CDMS Collaboration], arXiv:astro-ph/0203500.
35. R. Jakob, arXiv:hep-ph/0206271.
36. DAMA Collaboration, R. Bernabei *et al.*, *Phys. Lett. B* **436** (1998) 379.
37. J. Ellis, J. L. Feng, A. Ferstl, K. T. Matchev and K. A. Olive, *Eur. Phys. J. C* **24**, 311 (2002) [arXiv:astro-ph/0110225].
38. CDMS Collaboration, R. W. Schnee *et al.*, *Phys. Rept.* **307**, 283 (1998).
39. CRESST Collaboration, M. Bravini *et al.*, *Astropart. Phys.* **12**, 107 (1999).
40. H. V. Klapdor-Kleingrothaus, arXiv:hep-ph/0104028.
41. G. Jungman, M. Kamionkowski and K. Griest, *Phys. Rept.* **267**, 195 (1996);  
<http://t8web.lanl.gov/people/jungman/neut-package.html>.